Liquid water in the domain of cubic crystalline ice I_c

P. Jenniskens
The SETI Institute, 2035 Landings Drive, Mountain View, California 94043

S. F. Banham
School of Chemical Sciences, University of East Anglia, Norwich, Norfolk, NR4 7TJ, United Kingdom

D. F. Blake
NASA/Ames Research Center, Planetary Biology Branch, Mail Stop 239-4, Moffett Field, California 94035

M. R. S. McCoustra
Department of Chemistry, University of Nottingham, University Park, Nottingham, NG7 2RD, United Kingdom

(Received 16 August 1996; accepted 16 April 1997)

Vapor-deposited amorphous water ice, when warmed above the glass transition temperature (120–140 K), is a viscous liquid which exhibits a viscosity vs temperature relationship different from that of liquid water at room temperature. New studies of thin water ice films now demonstrate that viscous liquid water persists in the temperature range 140–210 K, where it coexists with cubic crystalline ice. The liquid character of amorphous water above the glass transition is demonstrated by (1) changes in the morphology of water ice films on a nonwetting surface observed in transmission electron microscopy (TEM) at around 175 K during slow warming, (2) changes in the binding energy of water molecules measured in temperature programmed desorption (TPD) studies, and (3) changes in the shape of the 3.07 μm absorption band observed in grazing angle reflection-absorption infrared spectroscopy (RAIRS) during annealing at high temperature, whereby the decreased roughness of the water surface is thought to cause changes in the selection rules for the excitation of O–H stretch vibrations. Because it is present over such a wide range of temperatures, we propose that this form of liquid water is a common material in nature, where it is expected to exist in the subsurface layers of comets and on the surfaces of some planets and satellites. © *1997 American Institute of Physics.* [S0021-9606(97)50628-3]

I. INTRODUCTION

When a thin layer of vapor-deposited amorphous water ice is warmed above 120–140 K (the glass transition temperature for amorphous water ice), it undergoes a transition from an amorphous solid to a viscous liquid.[1–3] The liquid form is thermodynamically distinct from liquid water[4–6] and exhibits a different temperature dependence of viscosity.[7,8] It has been called ''Water II'' by Speedy.[9] Recently, Johari *et al.*[10] presented evidence that its structure may depend somewhat on its history of formation, producing either liquid ''water A'' or ''water B''.

In earlier papers, this liquid form was considered to be of theoretical interest only and of little relevance in Nature, because amorphous water begins to crystallize to cubic ice soon after passing the glass transition temperature. However, crystallization is not complete and is effectively inhibited when only some 30% has transformed.[11,12] Hence, most of the ice persists as a viscous liquid in what has been called the ''restrained amorphous form''[12] between 140 and 210 K.

In this paper we will demonstrate that the restrained amorphous form (I_ar) is a liquid and that its liquid character persists into the cubic crystalline domain. Amorphous water ice exhibits marked changes in morphology when warmed above the glass transition, as a direct result of its rapidly changing viscosity. The observed morphological changes affect the surface area of the ice, the mean surface binding energy of the water molecules, the outgassing properties of impurities and, indirectly, the shape of the infrared absorption bands through changes in surface reflectivity properties.

The present article is organized as follows: In Sec. II, we describe the details of the experimental techniques. In Sec. III, we present the results. The observed phenomena are discussed in Sec. IV. We conclude that all of the observations are consistent with (and are a manifestation of) the decreasing viscosity of liquid water ice in the cubic crystalline domain. The presence of a liquid form of water ice in the cubic crystalline domain has important implications for the physical properties of naturally occurring ices in astrophysical environments.

II. EXPERIMENT

We have examined the structural and morphological properties of vapor-deposited amorphous water ice warmed into the cubic crystalline domain, between the maturation of crystallization and the onset of recrystallization to the hexagonal polymorph. We applied the techniques of grazing angle reflection-absorption infrared spectroscopy (RAIRS) and temperature programmed desorption (TPD) at the Universities of Nottingham and East Anglia, and transmission electron microscopy (TEM) at NASA/Ames Research Center. All these techniques utilize ice films of the same thickness prepared in nearly the same way.

The infrared absorption spectroscopy and temperature-programmed desorption experiments are carried out in an

ultrahigh vacuum ($< 10^{-8}$ mbar) chamber which has been described in detail elsewhere.[13,14] The infrared measurements are carried out on ultrathin (0.02 μm or 70 monolayer thick) ice films made by vapor deposition at a rate of 2.4 μm/h at pressures of 5×10^{-7} mbar onto a gold foil substrate held at 80 K. The temperature of the metal substrate, and hence that of the thin film, is controlled by resistive heating of the foil against the thermal sink of a liquid nitrogen reservoir. Temperatures reported herein are measured by a K-type thermocouple welded to the rear surface of the foil and are accurate to within $\pm$ 1 K. The infrared measurements are made in reflection-absorption geometry with a reflection angle of 75° from surface normal using a BioRad FTS60A-896 FTIR spectrometer and a liquid nitrogen cooled mercury cadmium telluride (MCT) photoconductive detector. The angle of reflection employed is rather less grazing than that commonly in use for RAIRS studies at the metal–vacuum interface, about 87°, and has been chosen to optimize sensitivity to the ice–vacuum interface.[14] The spectra reported herein have been¬ measured¬ over¬ the¬ wave¬ number¬ range 600–4000 cm^{-1} and represent ratios of 64 background (clean foil substrate) to 64 sample (foil substrate plus ultrathin ice film) spectra obtained during a total integration time of less than 5 min.

Temperature-programmed desorption (TPD) measurements are made with a computer-controlled quadrupole mass spectrometer (QMS, VG QX200). A temperature ramp of 50 K/min is applied to the substrate/ultrathin ice film and the evolved gas from the surface is monitored as a function of substrate temperature. In the current study, measurements were made of the H_2O^+ ion at a m/z of 18.

Bright-field imaging and electron diffraction studies of ice layers similar to those described above were carried out using a modified Hitachi H-500H transmission electron microscope (TEM). The instrument modifications necessary to perform low-temperature water ice experiments have been described elsewhere.[15,16] The ice layers are prepared as follows: An ultrathin (0.05 μm thick) water film is deposited *in situ* at a rate 20 μm/h from the vapor at 4×10^{-6} mbar onto an amorphous carbon film substrate supported by a copper grid cooled to 86 K. After deposition, the water vapor pressure is allowed to drop to the working pressure of the microscope (about 5×10^{-7} mbar). During subsequent warming, the confinement pressure increases to a few times 10^{-5} mbar. No increase in film thickness is observed during the experiments. The temperature of the substrate is controlled by resistive heating of the grid against the thermal sink of a liquid nitrogen Dewar. Changes in water structure are monitored by acquiring selected area electron diffraction patterns at a rate of several per minute during thermal annealing. In order to avoid beam damage, a different region of the water film is selected for each measurement and electron beam exposure is minimized. No changes in the water ice structure due to electron beam damage are observed on the time scale of individual measurements.

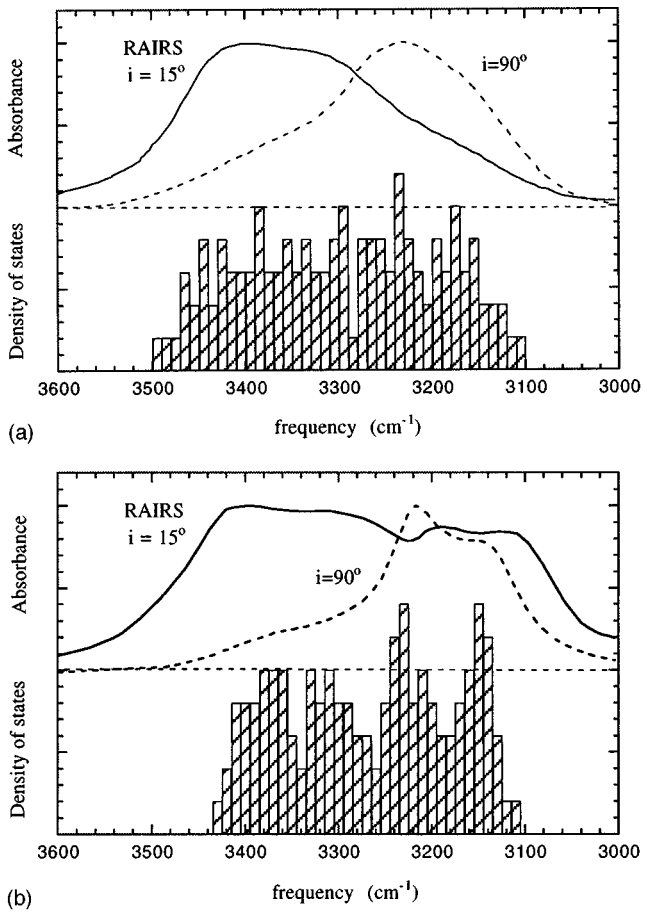

FIG. 1. (a) The 3 μm O–H stretch vibration band of low density amorphous water ice. The grazing angle RAIR spectrum of low-density amorphous ice at 80 K and the normal incidence ($i = 90°$) transmission infrared spectrum of Bergren *et al.* (Ref. 22) are compared to the theoretical density of states from the model by McGraw *et al.* (Ref. 23). (b) The O–H stretch vibration band of water ice in the cubic crystalline domain. As in (a). The RAIR spectrum after annealing at 160 K for 3300 s, and subsequent cooling to 80 K, is compared to the normal incidence transmission spectrum of Bergen *et al.* (Ref. 22) and the density of states from a model of cubic crystalline ice by McGraw *et al.* (Ref. 23).

III. RESULTS

A. Infrared absorption spectroscopy

Grazing angle RAIR spectra of submonolayer coverages of water ice on single crystal surfaces have been published previously.[17,18] Our results are from (by comparison) thicker layers and exhibit unexpected band changes during high-temperature annealing.

The RAIR spectra of ultrathin (0.02 μm thick) water films recorded at 80 K are consistent with other such RAIR spectra published in the literature,[19] but show significant differences when compared to the transmission spectra of thin (0.2 μm thick) films collected at normal incidence.[20–22] The results of these two techniques are compared in Figs. 1(a) and 1(b). Relative to transmission spectra, the RAIR spectra show an enhanced absorption at the high frequency end of the OH stretching region and a reduction in absorption intensity towards the lower frequency end. The result is a differ-

TABLE I. Vibrational assignments of the peaks and shoulders in the infrared spectra of (ultra-)thin and unannealed amorphous and crystalline H_2O films. Between brackets are the peak positions in ''deformed'' infrared spectra, either for relatively thick amorphous water films (1–10 μm thickness) or for annealed (3800 s at 160 K) partially crystallized ultrathin films (0.02–0.05 μm).

	Amorphous H_2O ($I_a l$)¬			Polycrystalline H_2O ($I_a r/I_c$)			
	Ultrathin RAIRS	(thick)	Thin Transmission (Refs. 20 and 22)	Unannealed RAIRS	(annealed)	Unannealed Transmission	(annealed) (Refs. 20, 22 and 45)
ν_1 (TO/LO)[a] out-of-phase	3410 s br¬	(3479 s br)	3367 sh¬	3381 sh¬	(3407 s)	3340 sh¬	(3360)
ν_3 (LO)	3307 sh¬	(3367 sh)	···	3305 s¬	(3305 sh)	···	
ν_3 (TO)	···	(3170 sh?)	3253 s¬	···	(3210 s)	3217¬	(3190)
ν_1 (TO/LO)[a] in-phase	3165 sh¬	(3158 s br)	3191 w¬	3158 sh¬	(3142 sh)	3149¬	(3135)
$3\nu_L$	2238 w br¬		2220¬	2239 w br¬		2235	
ν_2	1679 m br¬		1660¬	1647 m br¬		1604	
$2\nu_L$	1570 sh¬		1570¬	1544 sh¬		1570	
ν_L	890 s br¬		846¬	915 s br¬		833	

[a]LO/TO splitting for the symmetric modes is not large according to the LST relation, (Ref. 41) hence it is not possible to resolve the two bands. s—strong, m—medium, w—weak, br—broad, sh—shoulder.

ence in peak shape and peak position (3300–3400 cm^{-1} vs 3220 cm^{-1}). The positions of the peak and shoulders in the profile are listed in Table I. It is interesting to note that the spectrum calculated from theory[23] is intermediate in character with a centralized peak at 3290 cm^{-1}.

Crystallization results in a well-known sharpening of the infrared band, corresponding to a more ordered environment. During rapid warming of an ultrathin film of H_2O in steps of 10 K from 85 to 155 K, with annealing periods of up to 5 min at each temperature, no spectral changes were observed at temperatures up to 145 K. At 155 K spectral changes in the band are noted [compare Figs. 1(a) and 1(b)]. These spectral changes correlate with the onset of crystallization to cubic ice, as observed in thin, amorphous water ice films by electron diffraction.[8] Once again, the RAIR spectrum is characterized by significantly greater absorption at higher frequencies and a different absorption profile relative to spectra recorded in transmission mode.[22] The observed downward shift in position of the stretching vibrations as a function of increasing temperature (Table I) is known to be the result of stronger hydrogen bonding within the crystal. The absorption maxima also increase in intensity implying that a larger effective dipole moment exists as a result of increased molecular coupling in the more ordered environment. During warming from 80 K, the dangling O–H bond at 3692 cm^{-1} (not shown) disappears, marking an apparent reduction in the surface area of the film. This result is consistent with prior observations of the absence of this absorption band in crystallized films.[24]

An unexpected change of the infrared band shape was discovered during annealing at 160 K for extended periods. The band centered at 3381 cm^{-1} shifted to progressively higher wave numbers as a function of annealing time and an additional band at 3210 cm^{-1} was observed following annealing for 30 min. (Fig. 2). These changes are observed under conditions in which crystallization to the cubic ice polymorph should have been completed.[8] Figure 3 summarizes the peak positions of the four features in the band profile as a function of time in two high temperature annealing experiments.

The emerging infrared band bears some resemblance to the infrared band observed for water films that grow to a thickness comparable to the wavelength of the infrared light. The infrared spectra of relatively thick films of pure H_2O ice

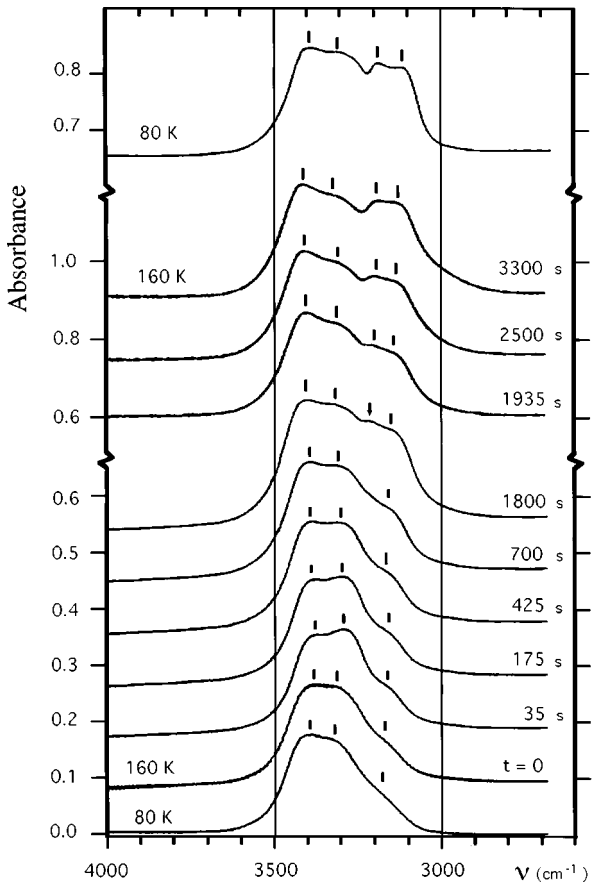

FIG. 2. Sequence of grazing angle RAIR spectra of the O–H stretch vibration band of water ice before, during, and after annealing at 160 K.

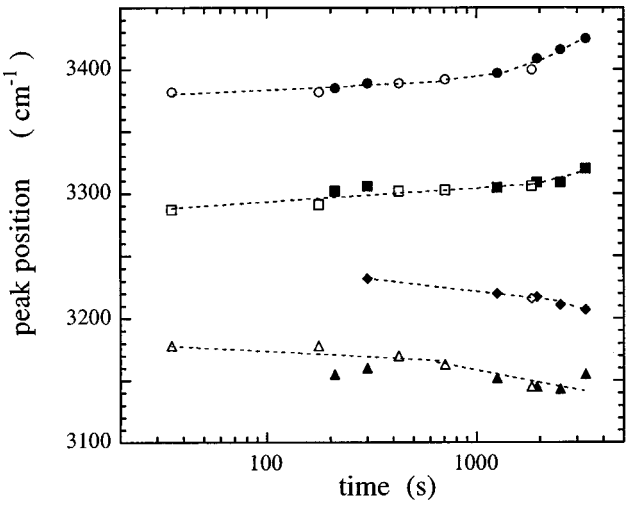

FIG. 3. The peak position of four maxima in the O–H stretch vibration band of water ice during annealing at 160 K in a compilation of two separate experiments from which spectra are shown in Fig. 2.

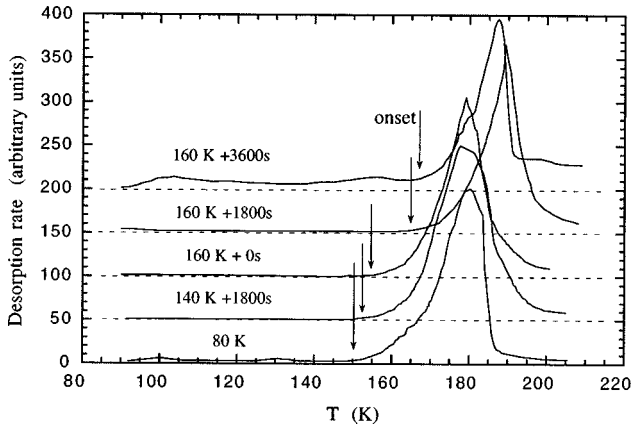

FIG. 5. Temperature programmed desorption (in arbitrary units) of water films that were annealed for various times at the indicated temperature and then cooled back to 80 K. The onset of desorption during a subsequent fast 50 K/min warmup is 15 K higher after annealing at 160 K.

deposited at 80 K were recorded for a succession of thicknesses (0.050–10 μm) and are shown in Fig. 4. The film thickness was estimated from the absorption intensity by comparison with the published transmission data of Koehler *et al.*[25] An increase in the thickness of the ice film by only a fraction of the wavelength of the infrared light results in the emergence of new bands at 3158 and 3479 cm^{-1} and a distorted band structure. The band changes resemble those seen during annealing at high temperature, although the central peaks are less pronounced. The effect cannot be a manifestation of the amorphous to crystalline transformation, which generally occurs at temperatures far greater than 80 K or in much thicker layers than 10 μm for the given deposition rate.[16] The infrared emission band peaks are not related to vibrational modes at the ice surface.[26] The various peak positions in the OH stretching region for both ultrathin and thick water ice films are summarized in Table I.

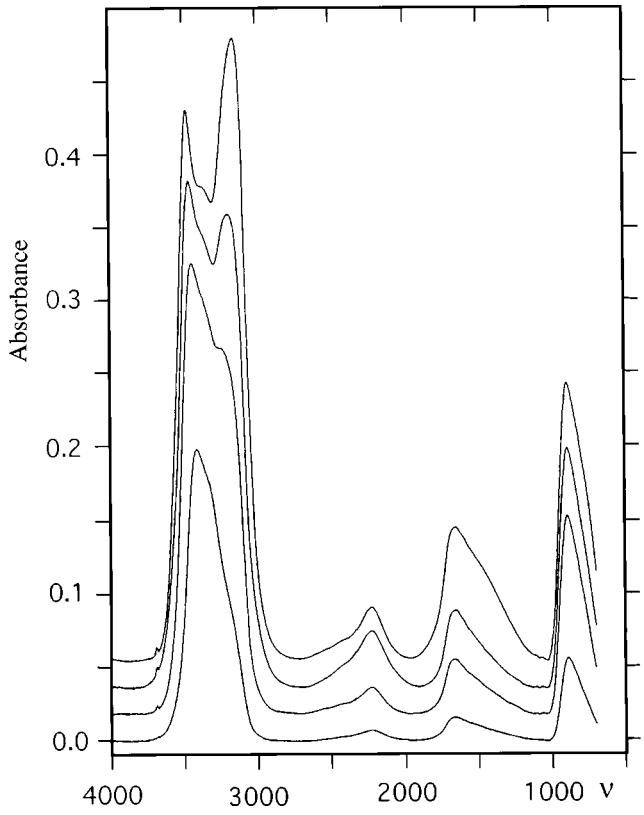

FIG. 4. RAIR spectra of thin water films for a succession of film thicknesses ranging from 0.050 μm at the bottom to 10 μm at the top (Ref. 43).

B. Temperature programmed desorption

Changes in the properties of water ice films before and after annealing are also observed during temperature programmed desorption experiments. The TPD measurements obtained from films annealed at 160 K under a confinement pressure of 1.10^{-7} mbar are shown in Fig. 5 and exhibit a shift of $+15\pm3$ K in the onset of desorption (from 152 $\pm$ 2 K to 167 $\pm$ 2 K) for annealing times of 30 min or longer. The temperature of maximum desorption is also increased, from 178 $\pm$ 2 K to 187 $\pm$ 3 K. The increase in the temperature of maximum desorption is indicative of more strongly bound water molecules at the surface of the film. Previous measurements[27] of the H_2O–H_2O surface binding energy H_s of fresh and annealed (3.5 h at 145 K) water films yield values of $H_s = 40.0 \pm 0.1$ kJ/mol and $H_s = 42.2 \pm 0.4$ kJ/mol, respectively. From a theoretical standpoint, this increase in surface binding energy between fresh and annealed water films should result in an increase in the temperature of desorption from 152 to 160 K. The given annealing time of 3.5 h at 145 K is equivalent to 0.14 h at 160 K. Our experiments show that for longer annealing times ($>$ 0.5 h at 160 K), the onset of desorption shifts to 167 $\pm$ 2 K, which corresponds to $H_s = 43.9 \pm 0.7$ kJ/mol.

C. Transmission electron microscopy

It was previously reported that viscous droplets (the ''crystallites'' in Jenniskens and Blake)[12] are formed during crystallization from the amorphous to the cubic crystalline

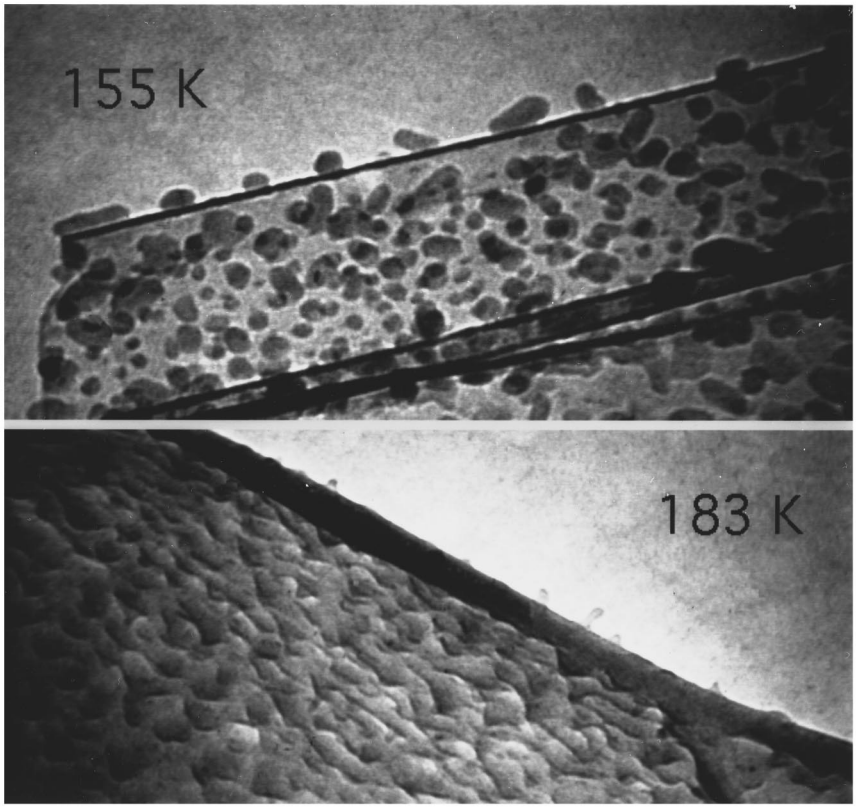

FIG. 6. Changes in the morphology of an ultrathin water film during a gradual warming are most apparent in these two images taken shortly after completion of crystallization (155 K) and at higher temperature (183 K) when the droplets flow into a more continuous morphology. The field of view of the upper figure is $\sim 8\ \mu$m, that of the lower figure is about 16 μm. The ice droplets are supported by a folded portion of the amorphous carbon film, resulting in a range of viewing angles.

state ($I_a \rightarrow I_c$).[8] These droplets protrude from the substrate surface to a height of 2 to 3 times the initial film thickness (Fig. 6, top). The process of droplet formation is complete when the rate of growth of the cubic crystalline pattern decreases abruptly at $\sim$ 163 K. The high contact angle of the droplets with the substrate ($\theta \sim 140°$) indicates that the specific surface free energy (γ) at the solid–liquid interface is very large,[28] where γ represents the difference in binding energy between surface and bulk molecules. The total surface area of the water–vacuum interface does not appear to change significantly; the formation of the viscous droplets is driven principally by the energetics of minimizing the surface contact area with the substrate.

Jenniskens and Blake[8] report that crystallization proceeds in two kinetic regimes. The first, due to crystal growth in individual domains, is marked by a rapid increase of the cubic (220) diffraction maximum, and occurs after an induction period determined by the rate of nucleation. The second is a more gradual increase limited by the nucleation rate in the remaining domains.[8] Diffraction and imaging studies show that small domains in the droplets crystallize, but that most of each droplet remains in an amorphous form. The amorphous fraction varies from droplet to droplet. The integrated intensity of the cubic (220) diffraction maximum increases to no more than 30% of the integrated intensity of the second amorphous diffraction maximum.[8] Complete nucleation does not occur prior to crystallization to hexagonal ice at a higher temperature or over a longer period of time.

Upon continued warming to 170–175 K, the well-defined droplets flow into a smoother morphology (Fig. 6, bottom), whereby the contact angle decreases to $\theta \sim 60°–80°$, a value that is more typical for liquid–water on graphitic surfaces ($\theta = 86°$ on graphite and $\theta = 72°$ on pyrolytic carbon).[28] Upon further warming, the layer retains somewhat irregular morphology. The change in morphology is not simply the result of sublimation, because the film thickness as measured from the diffracted intensity does not change significantly until just below 185–195 K. At this temperature the ice layer quickly sublimes in the $\sim 5 \times 10^{-5}$ mbar vacuum of the microscope.

The dramatic change in film morphology is accompanied by only a subtle narrowing of the cubic (111) and (220) diffraction maxima, suggesting that only minor changes in the distribution of the nearest-neighbor O–O distances and O–O–O bond angles have occurred. Most notably the broad wing of the (220) diffraction maximum gradually disappears. Figure 7, for example, shows the change of the diffraction pattern during annealing at 168 K for up to 20 h. Note that even after 20 h there is no sign of a hexagonal crystalline component. Hence, recrystallization from the cubic to the hexagonal crystalline polymorph ($I_c \rightarrow I_h$) does not occur during annealing on a time scale of tens of hours. Further-

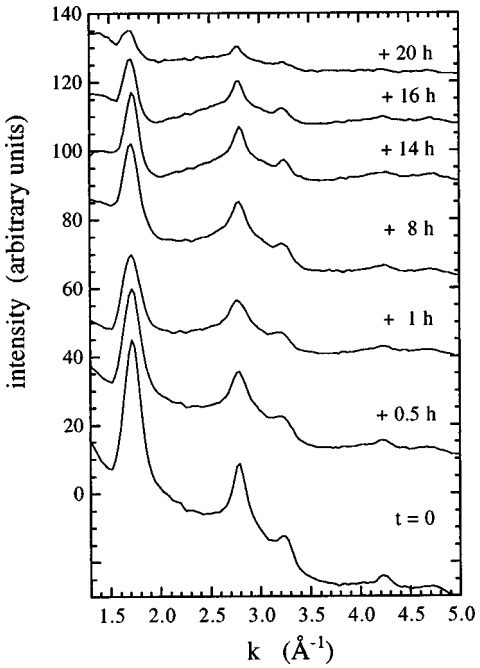

FIG. 7. Changes in the electron diffraction pattern of an ultrathin layer of water ice during annealing at 168 K after a gradual 1 K/min warm-up.

more, during gradual heating at 1 K/min, no sign of hexagonal crystalline ice is observed before the water layer has sublimed completely.

Diffraction peaks due the hexagonal crystalline polymorph are seen to emerge during long annealing at 160 K following a fast (34 K/min) warm-up from 86 K (Fig. 8). Bright-field imaging reveals that some droplets are well crystallized with numerous twinning planes. In experiments that include a rapid warmup shortly after deposition,[12] hexagonal

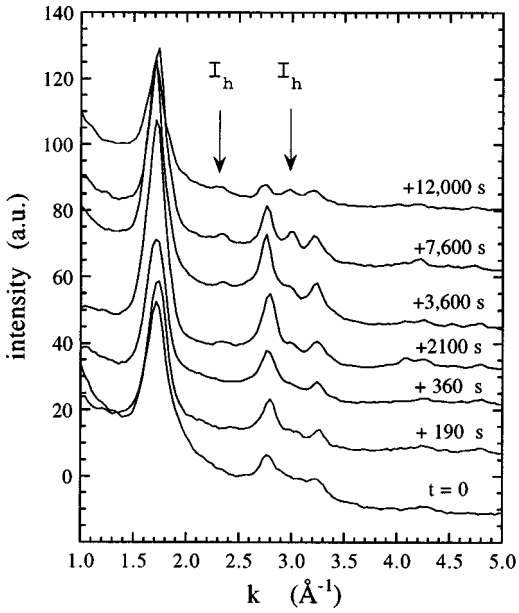

FIG. 8. Changes in the electron diffraction pattern during annealing at 160 K after a fast 34 K/min warm-up directly after deposition of an ultrathin ice layer at 86 K.

diffraction peaks appear along with the cubic diffraction peaks during crystallization, but the hexagonal component disappears upon continued gradual warming above 165 K. In all cases, the hexagonal domains are small and their emergence cannot account for the infrared absorption peak at 3210 cm^{-1} that appears during annealing at 160 after rapid warming. Infrared transmission and reflection spectra obtained for the cubic and hexagonal crystalline polymorphs I_c and I_h are identical within experimental error.[29,30] This is a consequence of the domination of the spectra by the strong coupling between oscillators and the average dipole moment in the two phases being identical.[31]

IV. DISCUSSION

A. The case for liquid water in the cubic domain

It is well established from differential thermal analysis that amorphous water ice films undergo a glass transition at about 120–140 K.[1,2] At this transition, increased thermal motion opens pathways to positional configurations that are kinetically inhibited at lower temperatures. Most likely, new molecular configurations are achieved through the movement of defects rather than through molecular diffusion, because diffusion is hindered in a fully hydrogen bonded network and the typical activation enthalpy is on average only two hydrogen bonds per molecule. This does not argue against the conclusion by Fisher and Devlin[32] that the glass transition is a manifestation of the onset of molecular rotation in the glass. Rather, by showing that the morphology of a thin film deposited on a nonwetting surface changes with temperature near the glass transition, we have demonstrated that passage through the glass transition temperature results in large-scale motion of the ice. The viscosity of the ice decreases above the glass transition, as is typical for other glassy materials, but the glass does not crystallize directly to the cubic polymorph as was previously believed.[32]

Jenniskens and Blake[8] studied the kinetics of the process of crystallization from the amorphous state and found that the relatively gradual increase of nucleation rate with temperature is consistent with the hypothesis that amorphous water ice above the glass transition is a strong liquid, as proposed by Angell.[7] The descriptor ''strong'' characterizes the temperature dependence of the viscosity, which decreases relatively gradually with increasing temperature above T_g following an Arrhenius law with a single activation energy barrier. In contrast, a ''fragile'' liquid such as normal liquid–water exhibits a rapid decrease in viscosity above the glass transition, often as much as ten orders of magnitude between T_g and 175 K.

Water can have a low viscosity only in the amorphous form. Cubic crystalline ice is a solid and does not flow. Indeed, x-ray and electron diffraction patterns[8,11,12] show that most of the diffracted intensity at temperatures between 155 and 210 K is due to an amorphous component that resists crystallization. Dark-field images reveal that crystallization of the original *low-density amorphous ice* $I_a l$ to the cubic crystalline polymorph I_c proceeds in small domains inside the liquid droplets. Each droplet contains numerous indi-

vidual crystals of irregular shapes embedded in the remaining amorphous *restrained amorphous form* I_ar (our notation).[12] The structure of I_ar is not fundamentally different from that of I_al, but is slightly more ordered. We speculate that I_ar consists of a subset of the initial configurations of I_al having an excess of hexagonal stacking order in small domains. We have argued that this short-range hexagonal stacking order prevents the amorphous form from crystallizing to the energetically favored cubic crystalline polymorph. Thus, I_ar coexists metastably with cubic ice until at higher temperature all water undergoes a reconstructive transformation into the hexagonal crystalline polymorph I_h.

We propose that the observed change in droplet morphology at high temperatures is a consequence of a progressive decrease in viscosity. This would be expected if a significant fraction of the water ice retains an amorphous form not greatly different from low-density amorphous ice below the glass transition temperature.

The observed decrease of the contact angle with the carbon substrate during the morphology change at 175 K cannot be caused by surface diffusion and recondensation. Some fundamental property of the water ice itself must be changing; otherwise the process would not change the contact angle of the water droplet with the nonwetting amorphous carbon substrate.

The contact angle θ is described by the Young equation[28]

$$\cos\theta=(\gamma_{sv}-\gamma_{sl})/\gamma_{lv}, \tag{1}$$

where ''s'' refers to solid, ''l'' to liquid, and ''v'' to vacuum. In order to explain the decreasing contact angles at 175 K, the binding properties of the water surface must be changing in such a way that the free energy of the solid–liquid interface γ_{sl} is decreasing, or the surface free energy at the ice–vacuum interface γ_{lv} is increasing, because the structure of the solid substrate (γ_{sv}) does not change during the experiment. The progressive increase of the onset of sublimation with annealing in our TPD experiments implies a decrease of surface free energy γ_{lv} (or increase of the H_2O–H_2O binding energy at the surface H_s), which cannot account for the smaller contact angle. Therefore, γ_{sl} must be decreasing, which implies a decreasing viscosity of the bulk ice. We observe that the contact angle θ approaches the value for that of normal liquid water in contact with an amorphous carbon substrate, in the limit of very low viscosity. We conclude that the morphology change observed at 175 K is due to the decrease of viscosity of the amorphous component, which persists well above the glass transition temperature.

At 170 K, the top few monolayers of the ice are rapidly restructured, during which time the amorphous material is expected to evaporate more rapidly than the solid crystalline material because amorphous and crystalline water desorb with activation energies of 46.9 and 48.3 kJ/mol, respectively.[33] Hence, the water might evaporate from the amorphous component and recondense in a crystalline form on the crystalline component. Indeed, the slight narrowing of the cubic (220) diffraction peak could suggest the expected growth of the crystals. However, the second diffraction maximum of the amorphous component does not decrease in amplitude in this temperature regime as would be expected, and there is no obvious growth visible in the darkfield images. Instead, some amorphous material must crystallize to cubic ice, as is evident from the corresponding heat release in differential thermal analysis (DTA) studies of water–ice films.[3,34,35] Figure 9 shows three typical DTA scans. Note that there are two regimes of heat release following the $I_a \rightarrow I_c$ transition. From x-ray diffraction data, it is known that the narrower of these regimes is due to the $I_c \rightarrow I_h$ recrystallization.[11,36,37] On the other hand, diffraction data do not support the interpretation[35] that the first, more shallow peak in DTA is due to $I_c \rightarrow I_h$ as well. Rather, this heat release coincides with the morphology change at 175 K which we interpret to be the result of crystallization of a small amount of amorphous ice. The total energy release in this regime is on the order of 100 J/mol, corresponding to an additional crystallization of only 7% of amorphous ice, given a heat release in the $I_a \rightarrow I_c$ transition of 1.35 kJ/mol.[33] Such a small heat release is consistent with the observed absence of cubic crystalline growth.

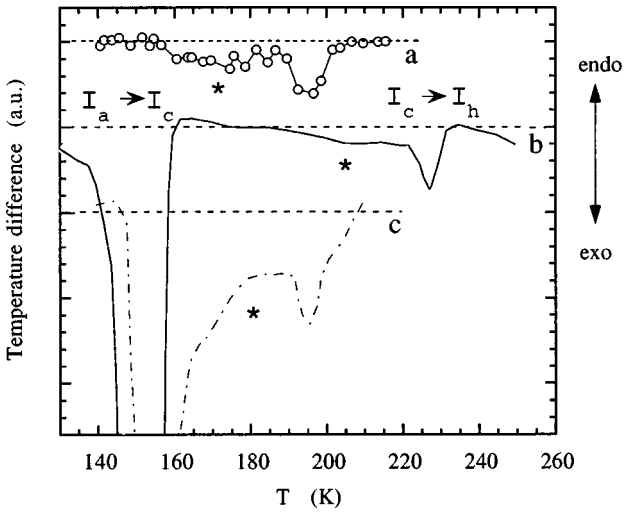

FIG. 9. Differential thermal analysis (DTA) scans of water ice films. Data are from: (a) Sugisaki *et al.* (Ref. 34) (b) Handa *et al.* (Ref. 35), and (c) Hallbrucker, Mayer and Johari (Ref. 3). The latter scan is similar to that shown by McMillan and Loss (Ref. 1). The first and last graphs refer to vapor deposited ice, the middle to pressure induced amorphous ice. Heating rates are 10, 0.17, and 10 K/min, respectively.

B. Changes in the infrared band shape

The observed change in the infrared band shape in this time-temperature regime is an indirect manifestation of this morphology change with potentially important implications for astrophysics, because infrared spectroscopy is used for remote sensing of astrophysical ices.

The infrared O–H stretch vibration band of water is difficult to interpret. Theoretical studies seem to result in reasonable distributions of densities of states (Fig. 1). Notably the four distinct peaks in the RAIRS spectra of annealed water films are reminiscent of the four peaks in the density of states of McGraw *et al.*[23] (Fig. 1). However, the calculation

of the oscillator strength of individual modes is difficult and the theoretical spectra do not match the observed spectra.

The band is extremely broad ($> 250\ cm^{-1}$) as a result of the anharmonicity of the vibrations generated by extensive hydrogen bonding within the ice. The spectra are dominated by intermolecular coupling between the oscillators. Hence, the vibrational modes do not have simple representations in terms of the symmetry of an individual water molecule ($C_{2\nu}$). Multiphonon/single phonon mixing analogous to Fermi resonance in the gas phase occurs between the ν_1 and the $2\nu_2$ modes and ν_2 and $2\nu_L$ resulting in the observation of the respective doublets with enhancement of the overtone bands. It should also be noted that due to the inherent disorder in amorphous ice, in addition to the strong intermolecular coupling, the peaks are not distinct.

In spite of the above, the normal mode assignments have been given in order to further the understanding of differences observed between transmission and reflection-absorption spectra as discussed below (Table I). These assignments are based upon a combination of Raman[38] and infrared spectroscopy,[22,39,40] theoretical predictions,[23] and the *Lyddane–Sachs–Teller* (LST) relation.[41] It has been shown that spatial periodicity is not required for the existence of *transverse optical* TO and *longitudinal optical* LO surface modes[42] and, therefore, TO and LO modes in ultrathin films may be observed in amorphous as well as crystalline materials. The LST relation describes the degree of splitting between the modes, which is proportional to the oscillator strength of the individual IR absorptions.

An explanation consistent with the spectral differences observed between the transmission and RAIR spectra of various layer thicknesses is provided by considering the optical effects arising from the vicinity of the substrate surface. The TO mode gives rise to a vibrational transition dipole moment parallel to the surface and is effectively neutralized by the so-called metal surface selection rule, whereas the LO mode has a surface–normal transition moment.

At grazing angles of incidence, the interference between the reflected and refracted rays results in a standing wave at the surface with $p_\perp$ polarization. Therefore, in close proximity to the metal surface only the LO modes can be excited. In normal incidence transmission spectroscopy, on the other hand, the LO modes can not be excited because of the complete absence of $p_\perp$ polarized radiation to which an LO mode can couple. Only the TO modes contribute to the spectrum. Hence, the observed differences between transmission and reflection-absorption infrared spectra from metal surfaces can be due to the excitation of TO and LO modes, respectively. The LO modes occur at higher frequency according to the LST relation and so the shift to higher frequency upon excitation of the LO modes is consistent with the observation of the OH stretching frequency distribution peaking at higher wave number in the RAIR spectra.

The effect of ice layer thickness on the RAIR spectra (Fig. 4) was recently studied using classical optical theory to simulate the RAIR spectra of water films of varying thicknesses up to about 4 μm.[43] It has been shown in these simulations that with increasing thickness of the film, to a thickness comparable to the wavelength of the infrared light, $p_\parallel$ (or s) polarized radiation is no longer effectively screened due to a breakdown in the metal surface selection rule and so it becomes possible to excite the TO modes. Hence, the increase in absorbance at lower frequencies with increasing thickness is a result of the excitation of TO modes in thicker films that can then couple with the fundamental vibrations.

Along similar lines of reasoning, one can postulate an explanation for the emerging infrared features of annealed ice films (Fig. 3). It is possible that, during the annealing process at 160 K, the surface in effect becomes more reflective due to a reduction in surface defects, resulting in a decrease in diffuse reflectance and increasing specular, that is mirrorlike, reflectance at the surface.[43] Specular reflectance increases the fraction of light reflected from the surface. Hence, the spectrum becomes more like the reflectance spectrum of a very thick layer (I_h has a sharp peak at $3233\ cm^{-1}$)[29] and is less affected by the metal surface selection rule. Specular reflectance is also especially strong at the center of the absorption band because of the link between the imaginary and real part of the complex refraction index.[44] This relationship can suppress the strength of the band at the peak relative to the wings and lead to band distortions. This effect may contribute to the measured differences between thick ice films at 80 K and annealed films at 160 K. We conclude that the observed IR band changes during annealing at high temperature are also a manifestation of the decreasing viscosity of water in the cubic domain above the glass transition temperature.

Although grazing-angle spectroscopy is not important for remote sensing of astrophysical environments, transmission infrared spectroscopy is. Therefore, it is of some interest that a similar emergence of an infrared band, though at a different wave number ($3135\ cm^{-1}$ vs $3210\ cm^{-1}$), has been reported by Schmitt *et al.*[45,46] Their experimental results concern the annealing of water-rich H_2O:CO_2 films. In their experiments, a Michelson FTIR beam was reflected from an aluminum metal substrate at normal incidence (Schmitt, private communication). A few experiments (20%–30%) were done in transmission at normal incidence, where the gas mixture was deposited on a cold KBr window and the infrared beam was reflected on an aluminium mirror directly behind the window. Schmitt *et al.*[45] went to great length to map the time-temperature dependence of the emerging feature, from which an activation enthalpy of 44.6 kJ/mol was derived (Fig. 10). This value is equal to that derived elsewhere for the process of crystallization.[8] Both crystallization and the morphology change at 175 K are expected to reflect the temperature dependence of the viscosity of the water, resulting in a similar activation energy.

The new feature described by Schmitt *et al.*[45] was assumed to be the fingerprint of cubic ice, but the O–H stretch vibration band of cubic ice does not normally exhibit this additional feature. Also, the feature emerges in the time-temperature diagram some 10 K higher than found on ultrathin films, but 13 K lower than the onset of the infrared feature in the RAIRS experiments. The latter discrepancy is more likely caused by the presence of the $CO_{(2)}$ impurity.

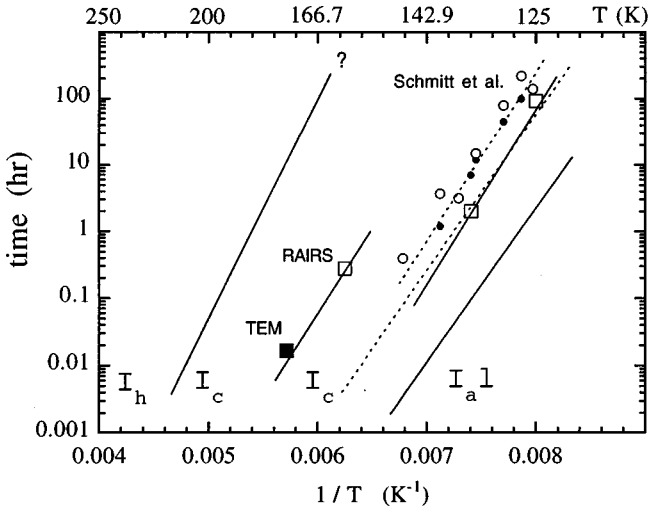

FIG. 10. A compilation of various structural changes in a time-temperature diagram. Various lines show the onset (—) and completion (···) of crystallization and the onset of recrystallization to hexagonal ice (—). These serve as a reference frame in which the onset of the emerging infrared bands in RAIRS and normal incidence transmission spectroscopy of Schmitt *et al.* (Ref. 45) are plotted by square symbols. The figure also reproduces from Schmitt *et al.* the data for the maturation of the emerging infrared band pattern (•) and the final release of CO and CO_2 (○).

Hence, we conclude that the emerging band is not a result of crystallization.

It is likely that the new band emerged due to changing illumination conditions. However, the different position of the new peak excludes the possibility that the TO/LO selection rules are changed. We note that the new peak at 3135 cm^{-1} is close to a second peak at 3137 cm^{-1} in the reflection spectra of hexagonal ice crystals by Ockman[29] and close to the Raman band at 3128 cm^{-1} assigned to the ν_1 in-phase stretching mode.[38] Although intramolecular coupling dominates the vibrational spectrum, the symmetric character of the modes varies across the profile[23] and the spectra suggest that there is a relative increase of excitation of symmetric modes over antisymmetric modes at later points in the annealing process. The thickness of the studied ice films were such that interference can have played a role and, again, an increasing reflectivity of the surface may have enhanced one type of mode over the other.

VI. SUMMARY

We conclude that a form of liquid water coexists with cubic ice in the temperature range 140–210 K. The principal evidence is: (1) the morphology of thin films deposited on a nonwetting surface changes with temperature (implying flow) as shown in electron microscope images, (2) a significant fraction of the sample in the cubic domain is amorphous as shown by electron diffraction patterns, and (3) desorption rates and infrared spectra of similar ice films are affected by annealing at high temperatures, indicative of the formation of smoother surfaces.

The morphology of ultrathin ice films on a nonwetting surface changes shortly after being warmed above the glass transition temperature (during crystallization at 142–165 K, when the ice film breaks into droplets), and again at about 175 K when the droplets flow into a smoother surface. The first observation provides the most direct evidence of a decreasing viscosity above the glass transition temperature, in which the ice minimizes its contact with the amorphous carbon substrate. The second is the result of a decreasing surface free energy at the liquid–substrate interface, implying a continuous decrease of viscosity up to at least 175 K in the cubic crystalline regime and above the temperature were crystallization to cubic ice has all but stopped. The alternative explanation, that the surface free energy at the water–vacuum interface increases, is not tenable based on arguments presented earlier. On the contrary, the surface free energy decreases, as is shown by the observation in temperature programmed desorption scans that annealing at 160 K has the effect of increasing the temperature of onset of sublimation by up to 20 K.

We have presented evidence that a viscous liquid form of water ice persists throughout the range of cubic crystallization, a relatively large temperature interval. This form of water can be common in natural environments, where it is expected to be present in subsurface layers of comets and the regolith of some icy planets. Earlier it was demonstrated that this form is a strong liquid, with different temperature dependence of viscosity than the fragile liquid water known at room temperature.

Infrared spectroscopy may allow the detection of this form of water in astrophysical environments by remote sensing. There are significant changes in the shape of the 3.07 μm infrared band in grazing angle RAIR spectroscopy during annealing at 160 K (with a confinement pressure of 1×10^{-7} mbar). A new band at 3210 cm^{-1} emerges, while other band positions change. We interpret these changes to be the result of a decrease in diffuse reflectance and an increase in specular reflectance, due to a morphology change, which results in an ice film that is optically flatter. Substrate surface selection rules result in selective excitation of specific vibrational modes, but are progressively weakened when the specular reflectance from the ice surface increases. A similar emerging band at 3135 cm^{-1} has been observed in transmission infrared spectroscopy by Schmitt *et al.* This band may have a similar origin, with a relative increase of excitation of symmetric modes over antisymmetric modes at later points in the annealing process and can perhaps be observed during remote sensing of astrophysical ices.

ACKNOWLEDGMENTS

P.J. and D.F.B. thank Gary Palmer for numerous modifications of the transmission electron microscope, which made this work possible, and Friedemann Freund for guidance. S.F.B. and M.R.S. McC. thank Andrew Horn, Michael Chesters, and Norman Sheppard for enlightening discussions on the topic of the infrared spectroscopy of water–ice and the United Kingdom Natural Environment Research Council for a research studentship (to S.F.B.) and equipment grant (to M.R.S. McC.). The work was initiated during a visit of P.J. to Nottingham University while a National Research

Council-ARC Research Associate, at the invitation of Peter Sarre. The current effort is supported by NASA funding from the Exobiology and Planetary Materials and Geochemistry programs and was performed under NASA Agreement NCC 2-572.

[1] J. A. McMillan and S. C. Los, Nature **206**, 806 (1965).
[2] M. Sugisaki, H. Suga, and S. Seki, Bull. Chem. Soc. Jpn. **41**, 2591 (1968).
[3] A. Hallbrucker, E. Mayer, and G. P. Johari, J. Phys. Chem. **93**, 7751 (1989).
[4] A. Rice, M. S. Bergren, and L. Swingle, Chem. Phys. Lett. **59**, 14 (1978).
[5] R. J. Speedy, Nature **380**, 289 (1996).
[6] H. Tanaka, Nature **380**, 328 (1996).
[7] C. A. Angell, J. Phys. Chem. **97**, 6339 (1993).
[8] P. Jenniskens and D. F. Blake, Astrophys. J. **473**, 1104 (1996).
[9] R. J. Speedy, J. Phys. Chem. **96**, 2322 (1992).
[10] G. P. Johari, A. Hallbrucker, and E. Mayer, Science **273**, 90 (1996).
[11] L. G. Dowell and A. P. Rinfret, Nature **188**, 1144 (1960).
[12] P. Jenniskens and D. F. Blake, Science **265**, 753 (1994).
[13] M. R. S. McCoustra and A. B. Horn, Chem. Soc. Rev. **23**, 195 (1994).
[14] S. F. Banham, Ph.D. thesis, University of East Anglia, Norwich, United Kingdom, 1995.
[15] D. F. Blake, G. Palmer, in *Analysis of Cometary and Interstellar Ice Analogs in the Electron Microscope*, edited by D. G. Howitt (San Francisco, California, 1991), p. 293.
[16] P. Jenniskens, D. F. Blake, M. A. Wilson, and A. Pohorille, Astrophys. J. **455**, 389 (1995).
[17] P. A. Thiel and T. E. Madey, Surf. Sci. Rep. **7**, 211 (1987).
[18] R. V. Kasza, K. Griffiths, V. P. Zhdanov, and P. R. Norton, Appl. Surf. Sci. **84**, 97 (1995).
[19] B. W. Callen, K. Griffiths, and P. R. Norton, Surf. Sci. Lett. **261**, 44 (1992).
[20] A. H. Hardin and K. B. Harvey, Spectrochem. Acta Part A **29**, 1139 (1973).
[21] E. Whalley, Can. J. Chem. **55**, 3429 (1977).
[22] M. S. Bergren, D. Schuh, M. G. Sceats, and S. A. Rice, J. Chem. Phys. **69**, 3477 (1978).
[23] R. McGraw, W. G. Madden, M. S. Bergren, S. A. Rice, and M. G. Sceats, J. Chem. Phys. **69**, 3483 (1978).
[24] B. Rowland and J. P. Devlin, J. Chem. Phys. **94**, 812 (1991).
[25] B. G. Koehler, L. S. McNeill, A. M. Middlebrook, and M. A. Tolbert, J. Geophys. Res. **980**, 10563 (1993).
[26] J. P. Devlin and V. Buch, J. Phys. Chem. **99**, 16534 (1995).
[27] S. A. Sandford and L. J. Allamandola, Icarus **76**, 201 (1988).
[28] A. W. Adamson, *Physical Chemistry of Surfaces*, 4th ed. (Wiley, New York, 1982), p. 4.
[29] N. Ockman, Adv. Phys. **7**, 199 (1958).
[30] J. E. Bertie and E. Whalley, J. Chem. Phys. **40**, 1637 (1964).
[31] P. V. Hobbs, *Ice Physics* (Clarendon, Oxford, 1974), p. 44.
[32] M. Fischer, J. P. Devlin, J. Phys. Chem. **99**, 11584 (1995).
[33] R. J. Speedy, P. G. Debenedetti, R. S. Smith, C. Huang, and B. D. Kay, Chem. Phys. **105**, 240 (1996).
[34] M. Sugisaki, H. Suga, S. Seki, in *Physics and Chemistry of Ice*, edited by N. Riehl, B. Bullemer, H. Engelhardt (Plenum, New York, 1969), p. 329.
[35] Y. P. Handa, O. Mishima, and E. Whalley, J. Chem. Phys. **84**, 2766 (1986).
[36] R. H. Beaumont, H. Chihara, and J. A. Morrison, J. Chem. Phys. **34**, 1456 (1961).
[37] J. E. Bertie, L. D. Calvert, and E. Whalley, J. Chem. Phys. **38**, 840 (1963).
[38] T. C. Sivakumar, S. A. Rice, and M. C. Sceats, J. Chem. Phys. **69**, 3468 (1978).
[39] W. Hagen, A. G. G. M. Tielens, and J. M. Greenberg, Chem. Phys. **56**, 367 (1981).
[40] W. Hagen, A. G. G. M. Tielens, and J. M. Greenberg, Astron. Astrophys. Suppl. Ser. **51**, 389 (1983).
[41] R. H. Lyddane, R. G. Sachs, and E. Teller, Phys. Rev. **59**, 673 (1941).
[42] A. Lehmann, Phys. Status Solidi B **148**, 401 (1988).
[43] A. B. Horn, S. F. Banham, and M. R. S. McCoustra, J. Chem. Soc., Faraday. Trans. **91**, 4005 (1995).
[44] O. S. Heavens, in *Optical Properties of Thin Solid Films* (Butterworths, London, 1955).
[45] B. Schmitt, R. Grim, and M. Greenberg, in *22nd Eslab Symposium on Infrared Spectroscopy in Astronomy* (ESA-SP 290 Salamanca Spain, 1989), p. 213
[46] B. Schmitt, S. R. J. A. Grim, J. M. Greenberg, and J. Klinger, in *Physics and Chemistry of Ice*, edited by N. Maeno and T. Hondoh (Hokkaido University Sapporo, 1992), p. 344.